

Gamma Driven Catalysis of Ammonia

September 2022

Samuel S Morrison
Lance R Hubbard
Caleb J Allen
Mark K Murphy
Samuel A Bryan
Amanda M Lines

DISCLAIMER

This report was prepared as an account of work sponsored by an agency of the United States Government. Neither the United States Government nor any agency thereof, nor Battelle Memorial Institute, nor any of their employees, **makes any warranty, express or implied, or assumes any legal liability or responsibility for the accuracy, completeness, or usefulness of any information, apparatus, product, or process disclosed, or represents that its use would not infringe privately owned rights.** Reference herein to any specific commercial product, process, or service by trade name, trademark, manufacturer, or otherwise does not necessarily constitute or imply its endorsement, recommendation, or favoring by the United States Government or any agency thereof, or Battelle Memorial Institute. The views and opinions of authors expressed herein do not necessarily state or reflect those of the United States Government or any agency thereof.

PACIFIC NORTHWEST NATIONAL LABORATORY
operated by
BATTELLE
for the
UNITED STATES DEPARTMENT OF ENERGY
under Contract DE-AC05-76RL01830

Printed in the United States of America

Available to DOE and DOE contractors from
the Office of Scientific and Technical
Information,
P.O. Box 62, Oak Ridge, TN 37831-0062
www.osti.gov
ph: (865) 576-8401
fox: (865) 576-5728
email: reports@osti.gov

Available to the public from the National Technical Information Service
5301 Shawnee Rd., Alexandria, VA 22312
ph: (800) 553-NTIS (6847)
or (703) 605-6000
email: info@ntis.gov
Online ordering: <http://www.ntis.gov>

Gamma Driven Catalysis of Ammonia

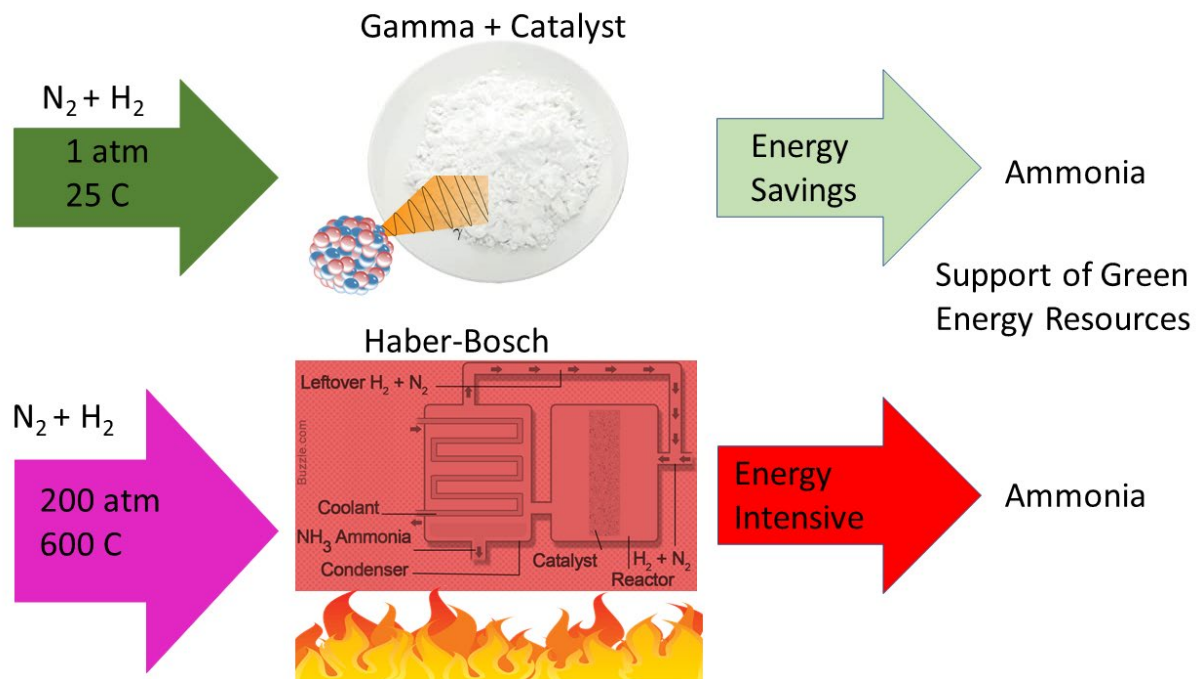
September 2022

Samuel S Morrison
Lance R Hubbard
Caleb J Allen
Mark K Murphy
Samuel A Bryan
Amanda M Lines

Prepared for
the U.S. Department of Energy
under Contract DE-AC05-76RL01830

Pacific Northwest National Laboratory
Richland, Washington 99354

Abstract



Experiments were conducted to investigate a passive production mechanism for the world's most energy intensive commodity, ammonia. A novel method, gamma catalyzed ammonia production at ambient conditions, was investigated. Ammonia is currently produced through the highly energy intensive Haber-Bosch process, which requires an operation pressure of 400 atmosphere and 600 degrees Celsius. Due to the high demand and need for ammonia, the Haber-Bosch process consumes 25% all energy produced globally. Reported herein was an attempt to produce ammonia at ambient temperature (20 C) and ambient pressure (1 atm), through a novel process developed at PNNL, gamma driven catalysis of ammonia. Although the measurements of the ammonia production suggest wild success, reports in the literature by Gao et.al. suggest an experimental positive bias in the results. To rule out the potential positive bias, multiple additional production campaigns would be needed to with an alternate analysis technique such as ion chromatography, as suggested by Gao et.al. Unfortunately, due to this late determination of potential positive bias, the results of this study remain inconclusive to the feasibility of gamma driven catalysis of ammonia and more work is needed to describe the chemical evolution with time. The results are a first step and demonstrate that gamma-catalyst mediated reactions are possible. This represents a key opportunity to explore the fundamental chemistry of high band gap catalysts that can change the paradigm of radiation, transforming it from a waste to a valuable energy source.

Acknowledgments

This research was supported by the Energy and Environmental Directorate (EED) Mission Seed, under the Laboratory Directed Research and Development (LDRD) Program at Pacific Northwest National Laboratory (PNNL). PNNL is a multi-program national laboratory operated for the U.S. Department of Energy (DOE) by Battelle Memorial Institute under Contract No. DE-AC05-76RL01830.

Acronyms and Abbreviations

Celsius (C)

Cobalt (Co)

Cobalt-60 (Co-60)

Hydrochloric Acid (HCl)

Ion selective electrode (ISE)

Iron (Fe)

Megapascal (MPa)

Part Per Million (ppm) is ($\mu\text{g/g}$ for solids) and ($\mu\text{g/mL}$ for liquids)

Sodium Hydroxide (NaOH)

Titanium (Ti)

Titanium Dioxide (TiO_2)

Ultraviolet (UV)

Contents

Abstract.....	ii
Acknowledgments.....	iii
Acronyms and Abbreviations.....	iv
1.0 Introduction	1
2.0 Method	3
2.1 Catalyst Synthesis	3
2.2 Catalyst Characterization	4
2.3 Gamma Irradiation	5
2.4 Post Irradiation Ammonia Quantification	8
3.0 Results and Discussion	10
3.1 Catalyst Analysis.....	10
3.2 Ammonia Production.....	12
3.3 Second Irradiation Campaign.....	14
3.4 Positive Bias from Side Product Reaction	18
3.5 Conclusion	19
4.0 References.....	20
Appendix: Ion Selective Electrode Incompatibility	23

Figures

Figure 1: Electrochemical reaction to produce ammonia via UV radiation from Zhao publication, (Zhao et.al., 2014).....	2
Figure 2: Synthesis series to produce the high band gap TiO ₂ doped Fe catalyst.	3
Figure 3: OMAX 40X-1600X Professional EPI-Fluorescence Trinocular Biological Microscope	4
Figure 4: Optima 5300 ICP-OES.....	4
Figure 5: Image of the 318 facility and the ⁶⁰ Co source utilized in the top left photo.	5
Figure 6: Image of the dose field from the ⁶⁰ Co source	6
Figure 7: Irradiation Setup for stainless steel vessels.....	7
Figure 8: Irradiation Setup for stainless steel vessels.....	8
Figure 9: Displayed is the UV Vis instrument (left), ion selective electrode (right)	9
Figure 10: Displayed are the catalyst after the final step for water removal.	10
Figure 11: Optical image of the titanium doped Iron doped catalyst.	11
Figure 12: Perceived production of ammonia without a catalyst.	15
Figure 13: Ammonia concentration for 900 ppm Fe in TiO ₂ catalyst both capped and uncapped with a nitrogen sparge.	16

Figure 14: Results from the 2 nd Irradiation Campaign in which the 900 ppm Fe in TiO ₂ catalyst for 5 g of catalyst in both stainless steel and glass vials.....	16
Figure 15: Results from the 2 nd Irradiation Campaign in which 40 mg of the 900 ppm Fe-TiO ₂ catalyst was evaluated for ammonia production in stainless steel vessels, and 40 mg of Fe-TiO ₂ in N ₂ gas spurge uncapped glass vials.	17
Figure 16: Results from the 2 nd Irradiation Campaign for the titanium catalyst in stainless steel vessels	17
Figure 17: Results from the Gao publication. “Photographs of different concentrations of ammonia solution (0, 0.4, 1.2, 2.0, 2.8, 4 mg/L). (a) Mixed with Nessler’s reagent. (b) Above ammonia solution containing 4 µg/L formaldehyde mixed with Nessler’s reagent. Light absorbance vs the ammonia concentration (red line) and ammonia solution with 4 µg/L formaldehyde (black line, c), 500 µg/L acetaldehyde (black line, d), and 80 µg/L acetone (black line, e).” (Gao et.al., 2018).....	18
Figure 18: Results from the ion selective electrode study looking at reproducibility of a single standard with multiple analysis is displayed.....	23

Tables

Table 1. Experiment sample list for the 2 nd irradiation campaign. Green are the blank samples, Black is the Iron Doped Catalyst, and Blue are the non-Iron Catalyst.....	7
Table 2. Concentration of Iron in the Titanium Dioxide Catalyst.....	11
Table 3. Cumulative dose calculated at each time interval of sampling for the first irradiation campaign.....	12
Table 4. Mass of catalyst in each vial examined	13
Table 5. Production of Ammonia at sampling intervals for each catalyst examined, in red are values that did not align with expectations, results are reported in µg/mL with instrumental uncertainty at < 10%.	14
Table 6. Cumulative dose calculated at each time interval of sampling for the second irradiation campaign	15

1.0 Introduction

Nuclear energy represents a key opportunity to meet green energy goals. However, high costs make nuclear energy uncompetitive on the market, ultimately discouraging deployment of reactors. However, by re-imagining how we utilize and deploy nuclear, we can not only improve the market standing of reactors but provide novel pathways to meet net zero goals and generate needed commodities without pulling energy from the grid. Currently, nuclear is primarily seen as a heat source; however, this viewpoint ignores a key energy source that is currently treated as a hazard and waste: radiation. New reactor designs and opportunities around off-gas capture mean we may be able to take advantage of radiation to drive chemical commodity production. This project begins to explore this opportunity with a key commodity. However, it should be emphasized that this proof-of-principle demonstration is primarily valuable as a pathway to characterize the fundamental chemistry of high band-gap catalysts. These highly oxidizing systems can exhibit impressive potentials and require high-energy excitement that can directly be supplied by gamma irradiation.

Ammonia is one of the most produced chemical commodities in the world, second to sulfuric acid (Valera-Medina et al., 2021). More than half of the ammonia produced is used in agriculture, making this commodity one of the most useful for feeding the entire world's population and paving the way for the last centuries growth during the industrial revolution (Fernandez & Hatzell, 2020). The production of ammonia is currently performed by the Haber-Bosch process, invented in the 1918. The process is very energy intensive, requiring high temperatures (400-600°C) and high pressure (20-40 MPa) to make this process viable (Wang et.al., 2021). The gamma process could lower the temperature and pressure of this reaction process, saving enormous amounts of energy.

As the current production of ammonia is energy intensive, a more economical, responsible, and elegant solution was sought to meet the need. Catalysts have been produced to lower the required production energy (Foster et al., 2018), but still require a driving force (Zhao et.al., 2014). Ultraviolet light has been shown to produce the types of reactions needed to ammonia production, but with low overall energy efficacy (Bao et.al., 2022).

Initial experimental conditions were developed based on prior art developed to produce ammonia utilizing ultra-violet photons (Zhao et.al., 2014). This seemed a natural progression as gamma radiation is a class of high energy photons. The Zhao publication synthesized Fe-TiO₂ nanoparticles that were utilized as the catalyst. The reaction mechanism of the catalyst and the reagent utilized 0.1% ethanol that was proposed by Zhao is displayed in Figure 1.

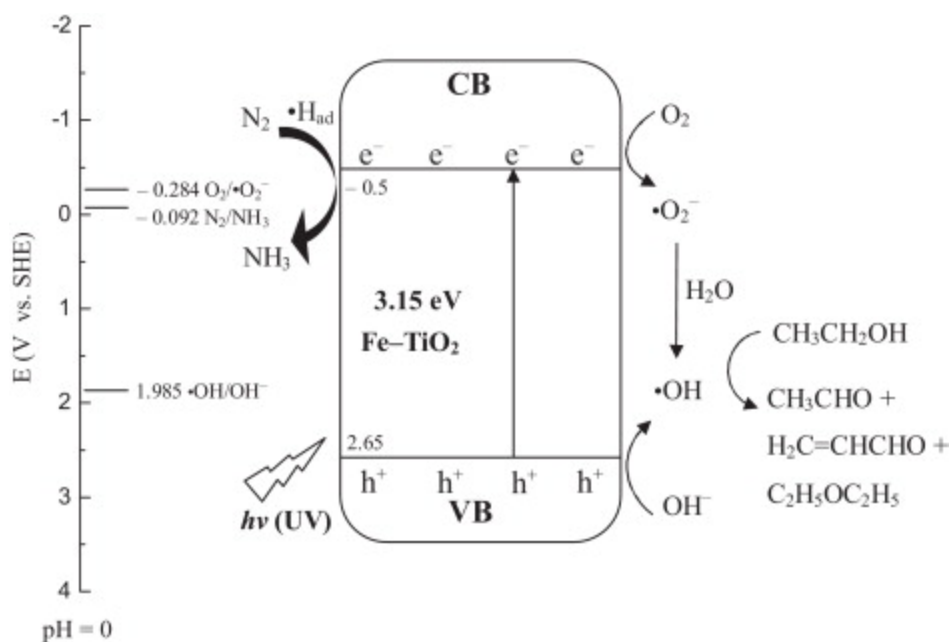


Figure 1: Electrochemical reaction to produce ammonia via UV radiation from Zhao publication, (Zhao et.al., 2014)

Experiments were conducted following the Zhao procedures for catalyst synthesis. Irradiation experiments were conducted using a cobalt-60 (Co-60) source available at PNNL.

2.0 Method

The research was conducted in series beginning with catalyst synthesis and characterization, followed by execution of the irradiation experiments, and performance was measured by ammonia quantitation at the end of the experiment.

2.1 Catalyst Synthesis

Synthesis of high band gap catalyst was performed following the method developed by Zhao et.al., with minor modifications. The iron doped nanoparticles were produced first by mixing 1.5 g of titanium dioxide (TiO_2) powder with 70 mL of 10 M sodium hydroxide (NaOH) and mixed for roughly 4 hours. The mixture was heated in a beaker for 48 hours in a Teflon beaker to dryness. The dried powder was rinsed with 0.1 M hydrochloric acid (HCl), and the solid was suspended in 40 mL of 18.2 M Ω -cm deionized water (DI) water. Enough hydrochloric acid was added to obtain a 0.1 M HCl solution. Iron (III) chloride in 0.1 M HCl was added in the appropriate concentration make the desired catalyst product. This solution as mixed for 24 hours, a diagram of the synthetic path of the Fe doped catalyst is displayed in Figure 2. An addition of 14 mL of DI water added and was allowed to stir for 2 hours. That solution was heated in a beaker to 180°C for 12 hours. The precipitate was filtered and rinsed with 100 mL of DI water, and finally dried for an hour at 80°C. A portion of the material was taken for imaging. The catalysts were then transferred to alumina crucibles and heated to 500°C for 4 hours, as described by Zhao as a calcining step.

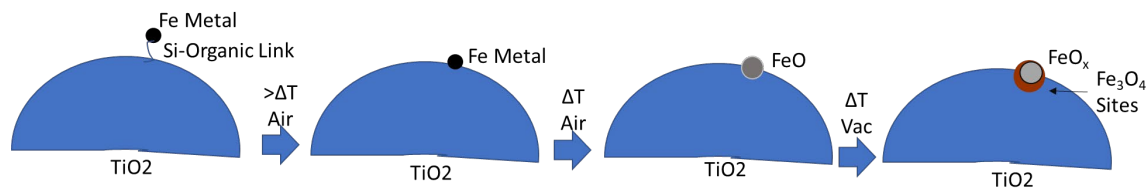


Figure 2: Synthesis series to produce the high band gap TiO_2 doped Fe catalyst.

A yellow-colored catalyst was prepared at roughly 100 ppm. The major difference in production between the Zhao method and the method that produced the yellow catalyst is the rate of the dry down. During production of the yellow catalyst the 48 hours dry down step was conducted in 4 hours and the catalyst visually changed color due to a charring effect. A quality assessment of the catalyst, to ensure quality was not affected through this production method.

An alternate rapid method of catalyst synthesis was developed for large scale catalyst synthesis. A solution of 500 mL of ethylene glycol had 100 g of titanium dioxide, that was heated to 200°C. Once the solution reached temperature, 1 gram of solid sodium hydroxide, 50 μL of 95% (3-mercaptopropyl)trimethoxysilane, and 127 mg of FeCl_2 was added. The solution was centrifuged at 100 rpm, and the ethylene glycol was washed off the precipitant with water. The precipitant was baked in an oven at 200°C for 12 hours. The rapid catalyst was then transferred to alumina crucibles and heated to 500°C for 4 hours.

Additional catalysts were investigated in which no synthesis was required, those catalyst included silicon dioxide (SiO_2), and aluminum oxide (Al_2O_3). A purely TiO_2 catalyst was

synthesized without the step in which Fe was added using the Zhao procedure and is described as a TiO₂ catalyst later in this report.

2.2 Catalyst Characterization

Catalyst was characterized by optical spectroscopy, instrument displayed in Figure 3, for qualitatively assessing the morphology of the catalyst. The imaging was performed prior to the calcining step for analysis. The reason the imaging was performed at this step was due to the flighty nature of the catalyst after the calcining step.



Figure 3: OMAX 40X-1600X Professional EPI-Fluorescence Trinocular Biological Microscope

For analysis of the iron content in the catalyst, inductively coupled-optical emission spectroscopy was performed, instrument displayed in Figure 4. The iron catalysts, roughly 10-30 mg per sample quantities were dissolved in a mixture of HCl and HF, due to the limited quantity of sample, dissolution was performed on single samples and heterogeneity was unaccounted for.



Figure 4: Optima 5300 ICP-OES

2.3 Gamma Irradiation

Irradiations were performed utilizing the gamma irradiation capability in the 318 building, displayed in Figure 5. Within the building is a 11,400 Ci source of Co-60. The source is lifted to the irradiator with the dose field displayed in Figure 6.



Figure 5: Image of the 318 facility and the ^{60}Co source utilized in the top left photo.

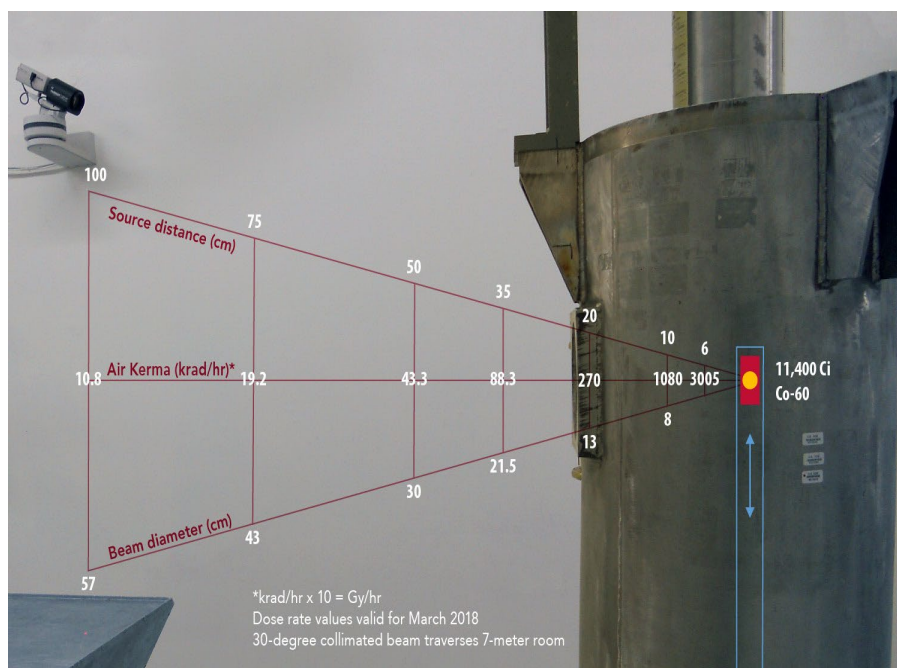


Figure 6: Image of the dose field from the ^{60}Co source

The experimental setup for the irradiation is displayed in Figure 7. Stainless steel vials were utilized in the initial irradiation campaign. Vials were filled with 40 mL of 0.1% ethanol solution in water, and 40 mg of catalyst, to match the Zhao publication (Zhao et.al., 2014). The samples were roughly 59.5 cm from the source set up in a fan array. Irradiations were conducted for a total of 19 hours with sampling at 30 minutes, 1 hour, 1.5 hours, 2 hours, 4 hours, and 19 hours. At each sampling 1 mL of solution was withdrawn from the stainless-steel vials. Note that the stainless-steel vessels were utilized for the initial irradiation campaign as there was concern that glass vials would not survive the initial irradiation.

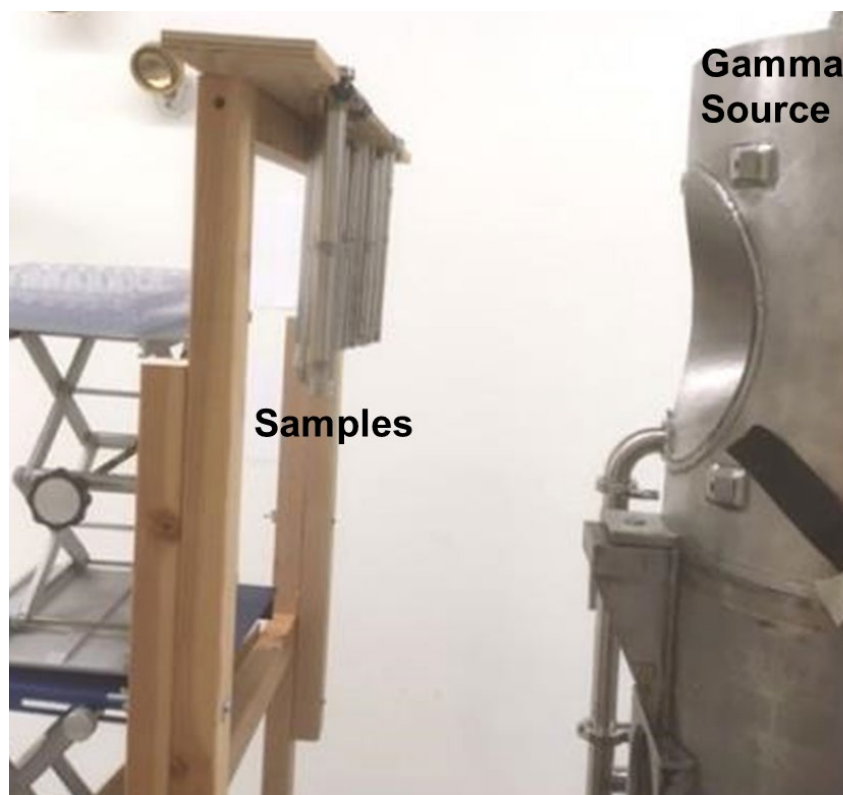


Figure 7: Irradiation Setup for stainless steel vessels.

Table 1. Experiment sample list for the 2nd irradiation campaign. Green are the blank samples, Black is the Iron Doped Catalyst, and Blue are the non-Iron Catalyst

blank: DI in SS	5g catalyst in SS, no sparge, no cap (A)	original mass catalyst, N2 sparge, no cap, in SS (A)	original mass catalyst, Ar sparge, no cap, in SS (A)
blank: ethanol in SS	5g catalyst in SS, no sparge, no cap (B)	original mass catalyst, N2 sparge, no cap, in SS (B)	original mass catalyst, Ar sparge, with septa, in SS (A)
blank: DI in glass	5g catalyst in glass, no sparge, no cap (A)	original mass catalyst, N2 sparge, with septa, in SS (A)	original mass catalyst, N2 sparge, no cap, in glass (A)
blank: ethanol in glass	5g catalyst in glass, no sparge, no cap (B)	original mass catalyst, N2 sparge, with septa, in SS (B)	original mass catalyst, N2 sparge, no cap, in glass (B)
5g TiO ₂ catalyst in SS, no sparge, no cap	40 mg TiO ₂ catalyst, Ar sparge, no cap, in SS	40 mg TiO ₂ catalyst, N2 sparge, no cap, in SS	40 mg TiO ₂ catalyst, N2 sparge, septa, in SS

A second irradiation campaign was conducted with a plethora of experimental conditions. Samples were run with gas being sparged into the vessels, alternate vessels were being examined (both quartz and stainless steel, and catalyst were being run in small size (40 mg) and large size (5g), rationale for each condition is included in the discussion below. The matrix for the experiment plan is displayed in Table 1. The setup for the 2nd irradiation is displayed in Figure 7 due to the setup for the irradiation the glass vials were placed on the exterior of the

portions of the irradiation field. As displayed some samples had either Argon (Ar) or Nitrogen (N₂) gas sparged into the mixture.

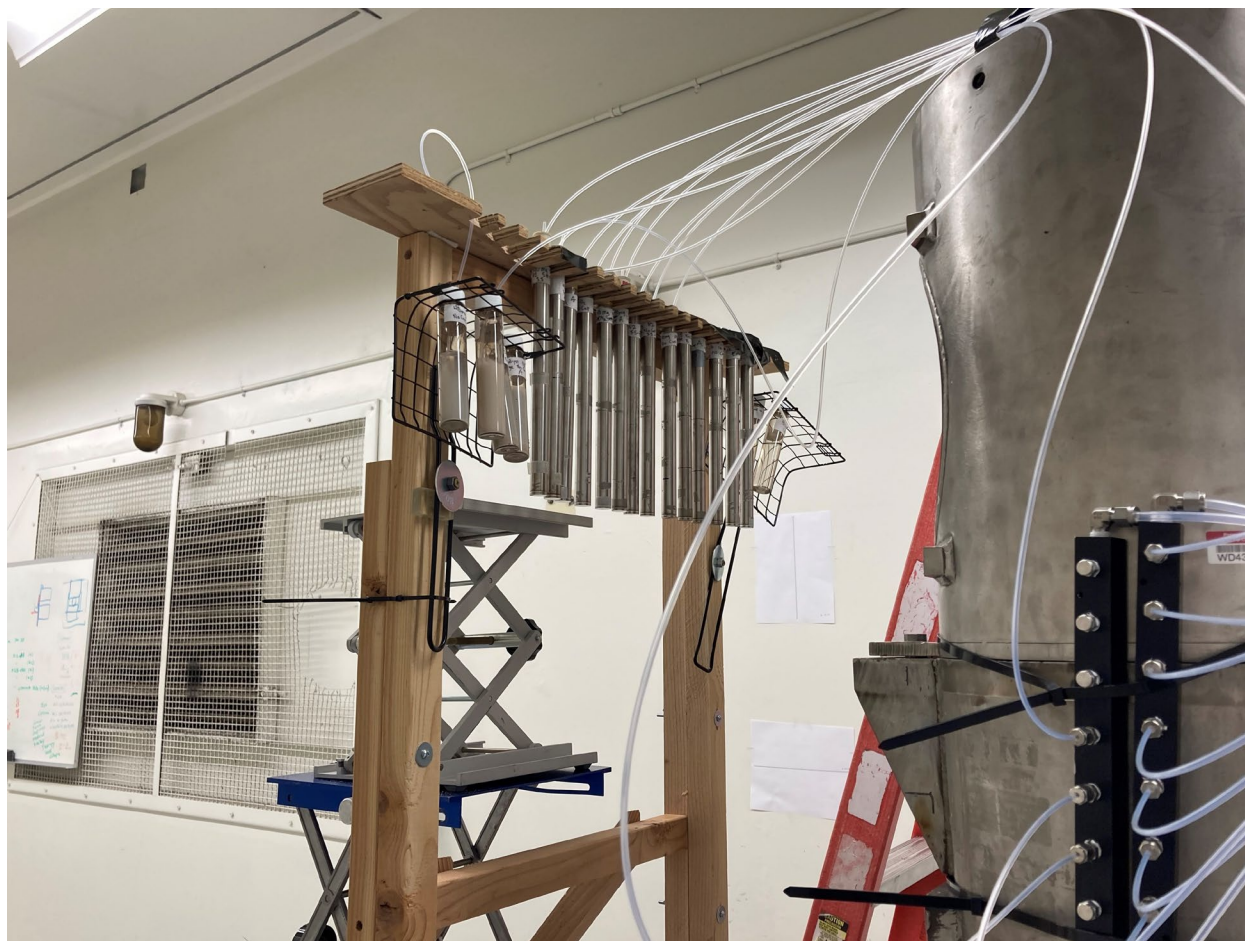


Figure 8: Irradiation Setup for stainless steel vessels.

2.4 Post Irradiation Ammonia Quantification

An assessment of methods for quantification of ammonia was performed. UV Vis was examined utilizing the Nessler's reagent reaction, and ion selective electrode was examined. The instrument models examined are displayed in Figure 9. The UV Vis analysis was performed by mixing Nessler's reagent (a mixture of potassium hydroxide and potassium mercury iodide) with the sample solutions. The reaction of ammonia with the mercury and iodide ions produces a red complex with absorbance at 420 nm, this absorbance scales as a function of ammonia concentration. An ion selective electrode was briefly examined, and the aqueous sample solution was found to be incompatible with the ion selective electrode, results displayed in Appendix: Ion Selective Electrode Incompatibility. All results reported herein were from UV Vis analysis.

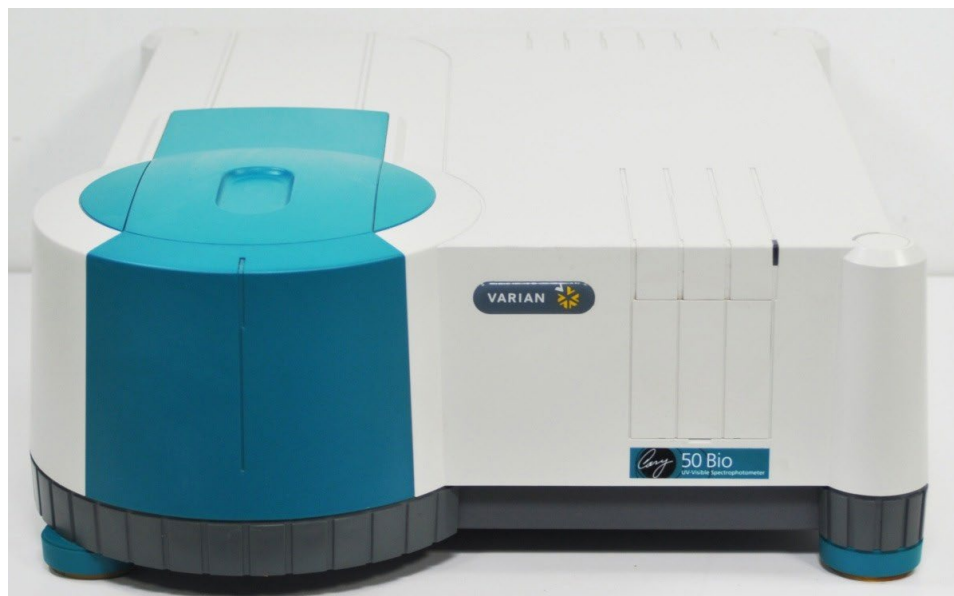


Figure 9: Displayed is the UV Vis instrument (left), ion selective electrode (right)

3.0 Results and Discussion

3.1 Catalyst Analysis

The produced catalysts are displayed in Figure 10. After the initial synthesis, in the final steps the catalysts were dried.



Figure 10: Displayed are the catalyst after the final step for water removal.

The catalyst that was synthesized was characterized by optical spectroscopy, see Figure 11. The morphology of the final product was rather heterogenous, with some particles greater than $20\ \mu\text{m}$. The figure displayed had roughly $800\ \mu\text{g}$ iron per gram of catalyst. Note that the microscope image was captured prior to the final drying step. One reason for this is that the catalyst powder becomes rather flighty after drying has been completed.

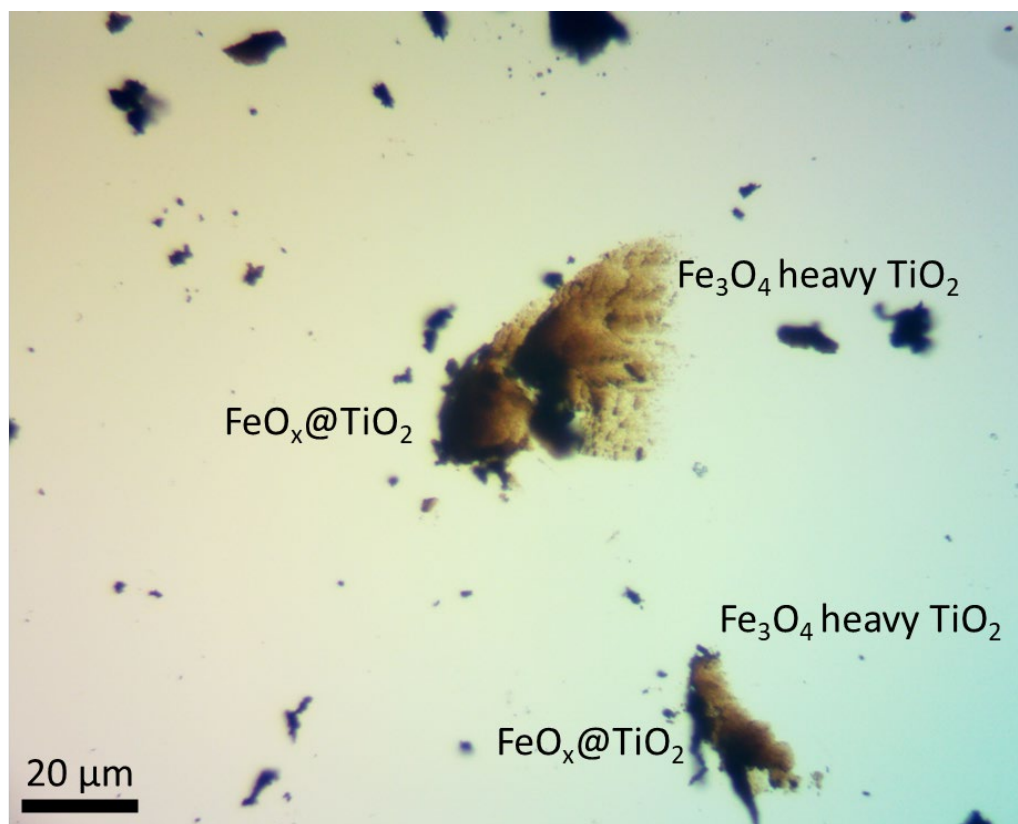


Figure 11: Optical image of the titanium doped Iron doped catalyst.

The quantity of iron in the catalyst examined was determined by ICP-OES. The concentration of Fe in the catalyst batches are displayed in Table 2. Note that to conserve catalyst, as the synthesis was non-trivial, a small quantity of catalyst was dissolved for analysis. Unfortunately, this led to a relatively larger uncertainty in the measurement and a non-detect for the lightweight Fe catalyst. The detection limit of the analysis accounts for the dilution of the sample and the mass of the catalyst dissolved.

Table 2. Concentration of Iron in the Titanium Dioxide Catalyst

Concentration of Fe in TiO ₂ Catalyst	Fe Conc (ug/g)
No Fe	< 0.9
Lightweight Fe	< 0.5
Featherweight Fe	49 ± 9
Welterweight Fe	80 ± 20
Yellow Welterweight Fe	84 ± 5
Middleweight Fe	170 ± 40
Cruiserweight Fe	460 ± 50
Heavyweight Fe	850 ± 60
Rapid Heavyweight Fe	900 ± 5

3.2 Ammonia Production

To establish a baseline for potential ammonia production without the enhancement of gamma catalysis, 40 mL of 0.1% ethanol was placed in the stainless-steel vessel and allowed to age. Aliquots were collected at 30 minutes, 20 hours, and 1 week. For each vessel the ammonia detected was below the quantification limit for the UV Vis analysis utilizing Nessler's reagent. Our conclusion from this experiment was that we do not have positive bias for our production solely from the initial starting reagent and vessel at least for over the course of a week.

Assessment for loss of ammonia to the atmosphere after irradiation was examined, 40 mL of 0.1% ethanol with 2.5 µg/mL of ammonia standard was run in triplicate. The solution was sampled after 30 minutes, 20 hours, and 1 week, the recovery of the ammonia was $91 \pm 2\%$, $94 \pm 2\%$, and $96 \pm 6\%$ respectively ($n=3$, $\pm 1\sigma$). Our conclusion from this experiment was that we did not have negative bias caused in the sample analysis time from sampling to instrument analysis as all samples were analyzed well within a week after irradiation.

The cumulative dose received for each sample solution for the first sample campaign is displayed in Table 3, with no dose received prior to irradiation.

Table 3. Cumulative dose calculated at each time interval of sampling for the first irradiation campaign

Irradiation Time Hours	Gamma Dose (Rad)
0.5	9650
1	19300
1.5	28950
2	38600
4	77200
19	366700

The mass of the catalyst examined for each vial in the irradiation is displayed in Table 4. Ideally each sample would have contained 40 mg of catalyst for the first irradiation campaign. This was a challenging task as the catalyst was loaded via spatula.

Table 4. Mass of catalyst in each vial examined

Label	Mass Catalyst (g)
No Catalyst-A	0
No Catalyst-B	0
SiO ₂ -A	0.0457
SiO ₂ -B	0.0417
TiO ₂ -A	0.0447
TiO ₂ -B	0.0434
Al ₂ O ₃ -A	0.0399
Al ₂ O ₃ -B	0.0401
Yellow 80 ppm FeTiO ₂ -A	0.0394
Yellow 80 ppm FeTiO ₂ -B	0.0361
80 ppm FeTiO ₂ -A	0.0420
80 ppm FeTiO ₂ -B	0.0448
500 ppm FeTiO ₂ -A	0.0357
500 ppm FeTiO ₂ -B	0.0457
Rapid 900 ppm Fe-TiO ₂ -A	0.0419
Rapid 900 ppm Fe-TiO ₂ -B	0.0405

The production of ammonia within each vessel is displayed in Table 5. Note that for the sampling performed at 4 hours and 19 hours for the SiO₂ sample-B the values were substantially lower than expected. Currently, we have unconfirmed hypothesis of improper sampling, with no evidence to prove or disprove that conclusion. One of the major discoveries from the irradiation was that the no-catalyst sample which contained 0.1% ethanol, had production of ammonia. The evidence of the production of the ammonia in vessels without catalyst, is likely evidence that the vessel itself is acting a catalyst. Further discussion is included below.

Table 5. Production of Ammonia at sampling intervals for each catalyst examined, in red are values that did not align with expectations, results are reported in $\mu\text{g}/\text{mL}$ with instrumental uncertainty at $< 10\%$.

Time (Hr.)	0	0.5	1	1.5	2	4	19
No Catalyst-A	<1	<1	1.5	1.6	2.2	5.0	17.3
No Catalyst-B	<1	<1	1.1	1.5	1.9	5.4	17.2
SiO ₂ -A	<1	<1	1.0	1.5	2.1	4.2	18.0
SiO ₂ -B	<1	<1	1.2	1.7	2.3	2.7*	8.2*
TiO ₂ -A	<1	<1	<1	2.0	3.7	4.6	16.2
TiO ₂ -B	<1	<1	1.2	1.8	2.5	4.6	16.9
Al ₂ O ₃ -A	<1	<1	<1	1.6	2.0	4.6	15.5
Al ₂ O ₃ -B	<1	<1	<1	1.4	1.7	3.7	16.7
Yellow 80 ppm FeTiO ₂ -A	<1	<1	<1	1.8	2.2	4.0	14.2
Yellow 80 ppm FeTiO ₂ -B	<1	<1	<1	1.8	2.3	5.0	18.8
80 ppm FeTiO ₂ -A	<1	<1	1.1	<1	2.3	4.3	15.1
80 ppm FeTiO ₂ -B	<1	<1	<1	1.5	2.0	5.4	15.0
500 ppm FeTiO ₂ -A	<1	<1	1.2	1.9	2.4	4.5	17.6
500 ppm FeTiO ₂ -B	<1	<1	1.1	1.5	2.1	4.9	15.9
Rapid 900 ppm Fe-TiO ₂ -A	<1	<1	1.1	1.8	2.7	5.2	19.2
Rapid 900 ppm Fe-TiO ₂ -B	<1	<1	<1	1.6	2.3	4.5	20.3

*Values outside of expectation

3.3 Second Irradiation Campaign

A second irradiation campaign was pursued with little funding remaining and lots of ideas. The 2nd irradiation campaign was pursued with an investigation of saturation point for ammonia. The ammonia production, as ppm, was analyzed for each of the irradiated samples, in the various conditions. The results from these analyses are included in Figure 12 through Figure 16. For the second irradiation campaign, the sample dose is included in Table 6 for 15-42 hours production.

Table 6. Cumulative dose calculated at each time interval of sampling for the second irradiation campaign

Irradiation Time Hours	Gamma Dose (Rad)
15	289500
22	424600
38	733400
40	772000
42	810600

To assess the potential role of stainless steel as an alternative source of catalysis for the ammonia production reaction, a comparison of stainless-steel vessel and glass vessels under irradiation was done. Single samples of di-ionized water or 0.1% ethanol were run in either glass or stainless-steel vessels. The results of those samples are displayed in Figure 12. These results contended our initial hypothesis that the stainless-steel vessel was acting as a catalyst, as the ammonia production occurred with the ethanol solution. Furthermore, it is inconclusive whether glass is behaving in a catalytic fashion like the SiO₂ catalyst discussed above. Another potential avenue for the ammonia production may be through direct gamma driven production, requiring only the ethanol. Without further confirmation it is difficult to provide concrete conclusions.

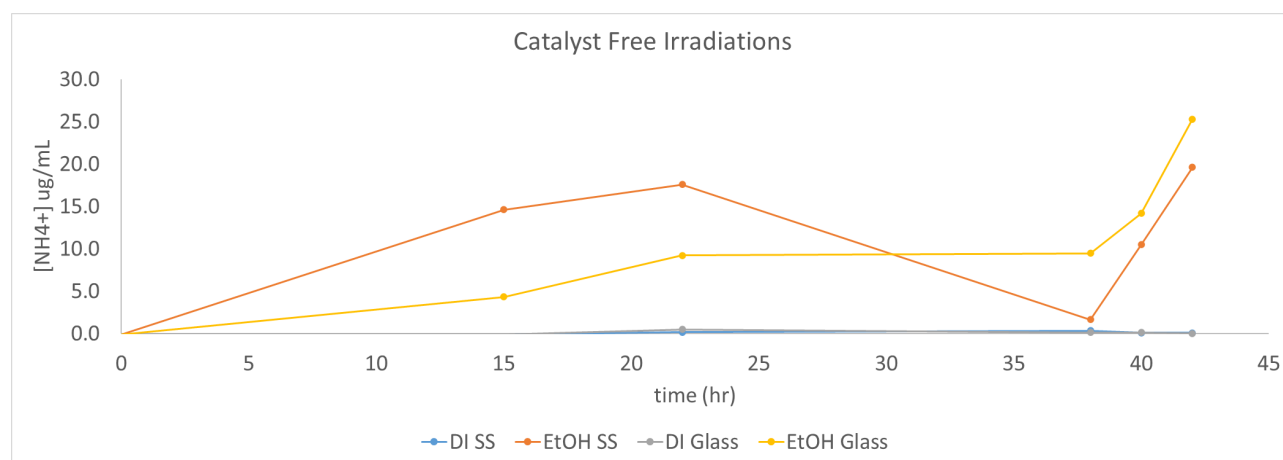


Figure 12: Perceived production of ammonia without a catalyst.

The effects of an open atmosphere during the irradiation were investigated, comparing a capped and uncapped vessel examining the production of ammonia. The result of this investigation is shown in Figure 13.

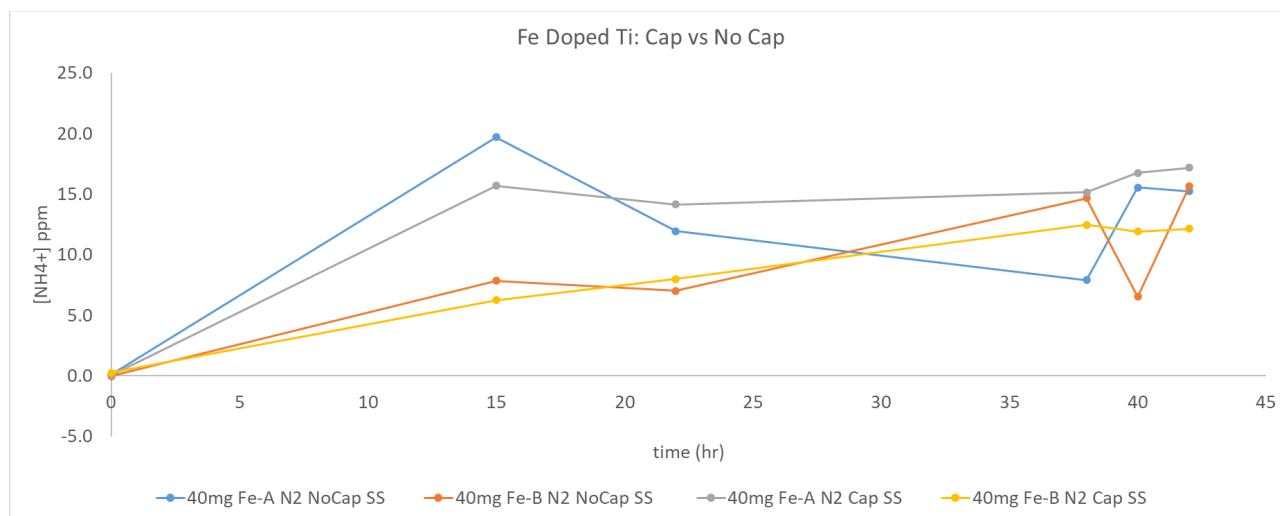


Figure 13: Ammonia concentration for 900 ppm Fe in TiO₂ catalyst both capped and uncapped with a nitrogen sparge.

The contribution of the stainless-steel vessels was assessed with 5 g of 900 ppm Fe-TiO₂ catalyst. The samples were not sparged with a gas and the samples were open to atmosphere like the first irradiation campaign, with a larger quantity of catalyst, results displayed in Figure 14. The results of the 2nd irradiation campaign show indistinguishable difference between the results of the stainless-steel vial and the glass vial.

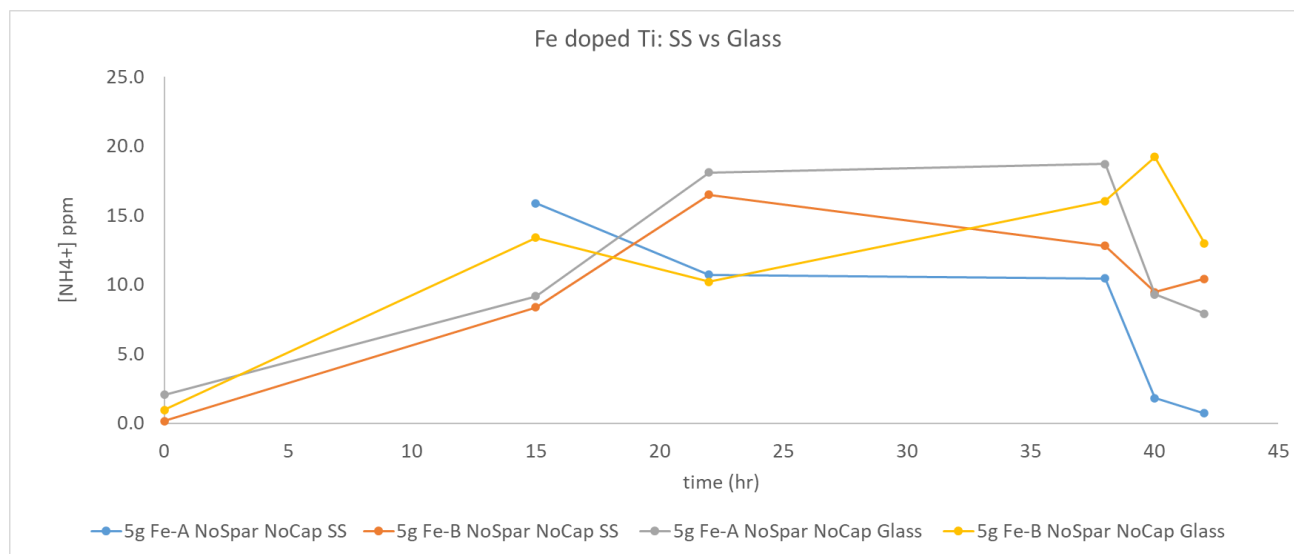


Figure 14: Results from the 2nd Irradiation Campaign in which the 900 ppm Fe in TiO₂ catalyst for 5 g of catalyst in both stainless steel and glass vials.

An assessment of the impact of catalyst suspension was investigated with sparging argon (Ar) or Nitrogen (N₂) into the vials. The Ar was hoped to be useful for suspending the resin as to ensure that the catalyst would not solely sit on the bottom of the vessel. The results of this assessment are displayed in Figure 15. Note that in comparison of the nitrogen spurge glass 40

mg vial in glass Figure 15 and in stainless steel in Figure 14 suggest that the stainless-steel vessel has a net positive effect for the perceived production of ammonia.

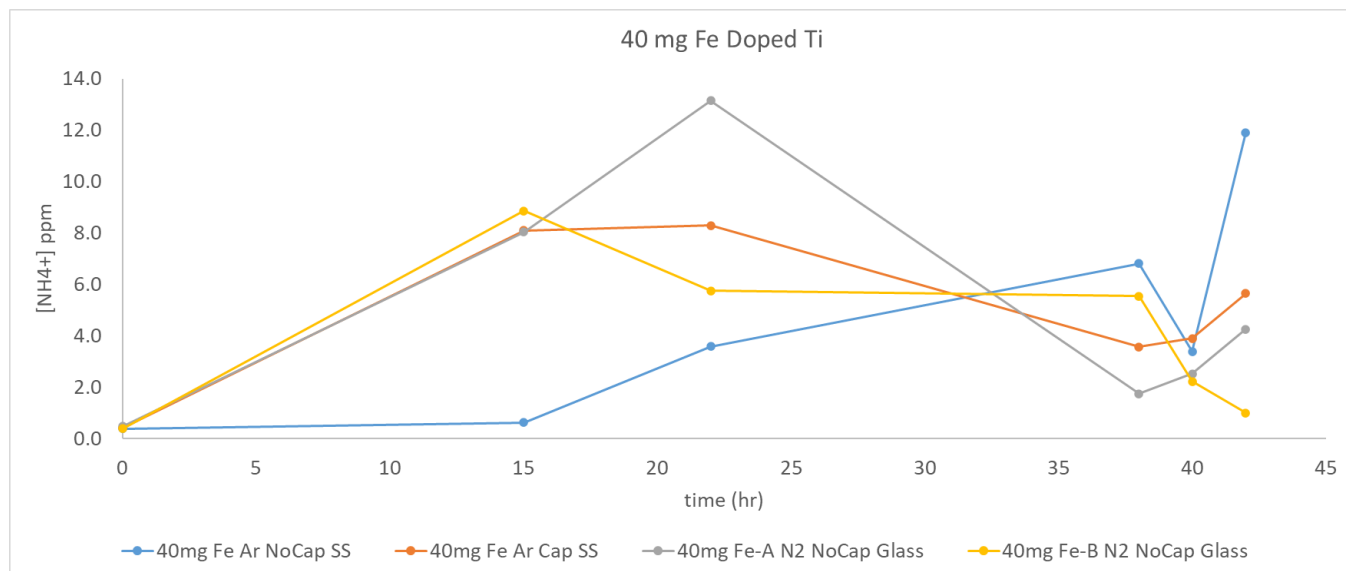


Figure 15: Results from the 2nd Irradiation Campaign in which 40 mg of the 900 ppm Fe-TiO₂ catalyst was evaluated for ammonia production in stainless steel vessels, and 40 mg of Fe-TiO₂ in N₂ gas spurge uncapped glass vials.

Titanium only catalysts were examined in stainless steel vessels. One sample was analyzed with 5 g of the TiO₂ catalyst. The other 3 samples had 40 mg of the TiO₂ catalyst with argon, catalyst with nitrogen capped, and catalyst with nitrogen uncapped. The results are displayed in Figure . Note that the titanium sample with the 5 g of catalyst exceeded production rates of all other conditions, including the results from the first irradiation campaign.

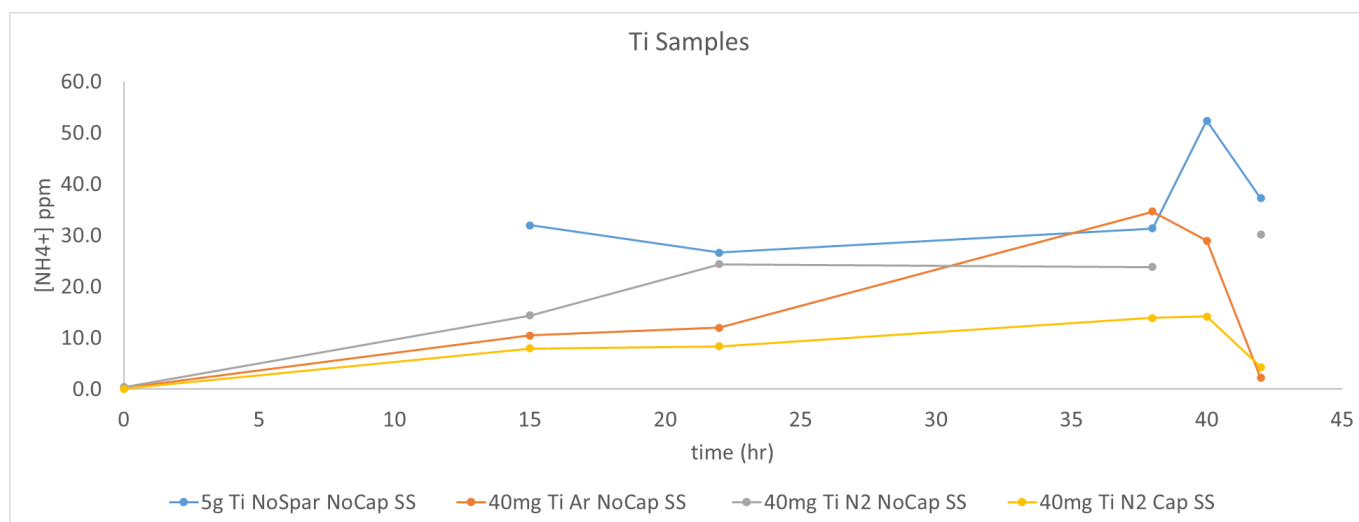


Figure 16: Results from the 2nd Irradiation Campaign for the titanium catalyst in stainless steel vessels

In summary of the results of the second irradiation campaign, the 0.1% ethanol solution without catalyst, even in the glass vials, had ammonia detected in the solution. The most rapid rate of

production observed was the 5g of TiO_2 in the stainless-steel vessel without a cap and the solution had no sparge. The purely DI water samples had no ammonia detected in the solution.

3.4 Positive Bias from Side Product Reaction

At the conclusion of the project as the results were being pulled together a team member discovered through a deep dive into the literature, a pathway for positive bias. In the method of ammonia production, a sacrificial reductant ethanol, was needed to produce ammonia. The publication by Gao et.al. states that side products of formaldehyde, acetaldehyde, and acetone are produced through this reaction. In the Gao publication, a comparison of ammonia quantification by ion chromatography versus UV-vis and Nessler's reagent displayed ammonia recoveries 70-fold higher than results determined by ion chromatography. Displayed in Figure 17 are the results of the Gao study. In rough summary trace production of byproducts from ethanol result in a substantial positive bias in analysis through UV-vis via the Nessler's reagent process. To truly validate the results of this study, analysis by ion chromatography or other direct measurement of ammonia such as ion selective electrode, is the only viable pathway for clear results. It is the recommendation of this team that these results be taken as inconclusive until an additional irradiation campaign is conducted, and analysis is conducted via ion chromatography.

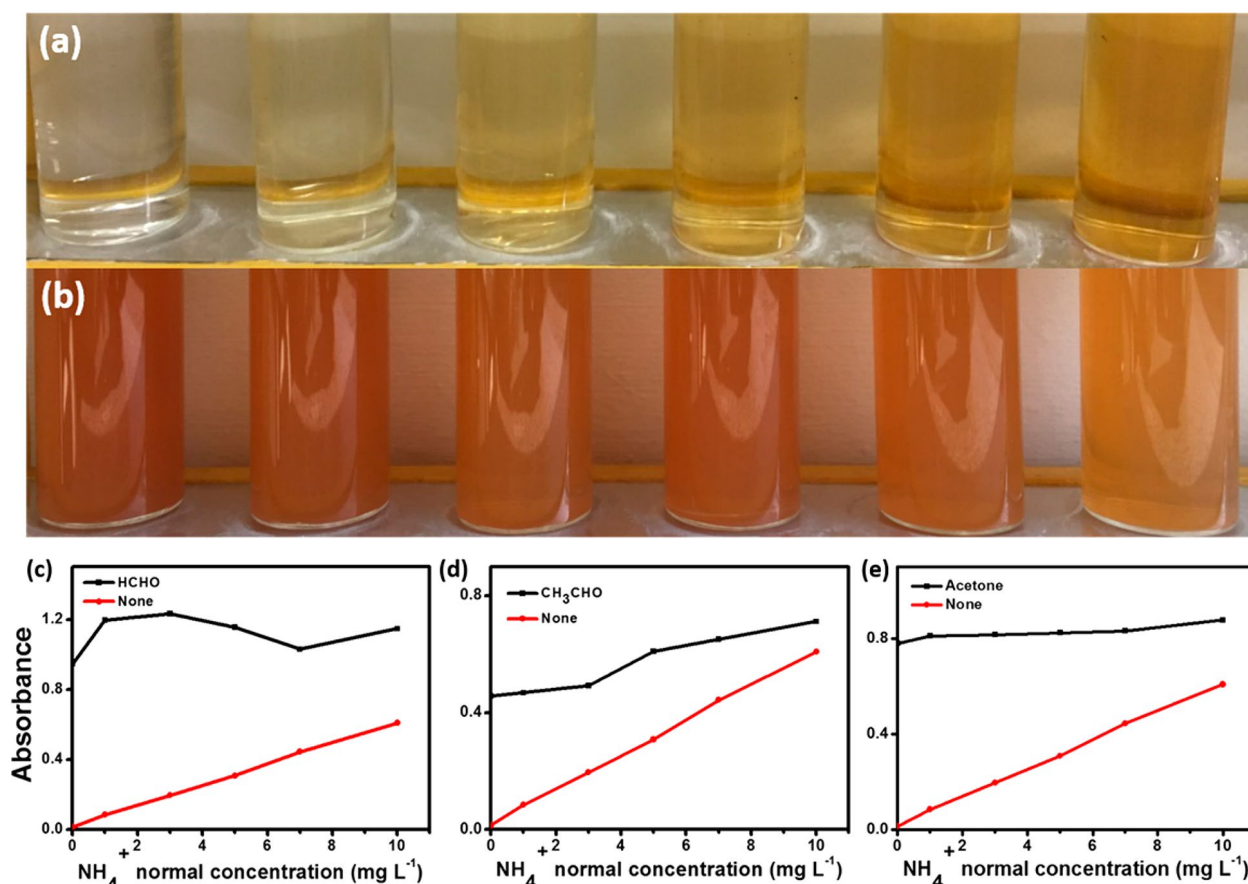


Figure 17: Results from the Gao publication. "Photographs of different concentrations of ammonia solution (0, 0.4, 1.2, 2.0, 2.8, 4 mg/L). (a) Mixed with Nessler's reagent. (b) Above ammonia solution containing 4 µg/L formaldehyde mixed with Nessler's reagent. Light absorbance vs the ammonia concentration (red line) and ammonia solution with 4 µg/L

formaldehyde (black line, c), 500 $\mu\text{g/L}$ acetaldehyde (black line, d), and 80 $\mu\text{g/L}$ acetone (black line, e)." (Gao et.al., 2018)

3.5 Conclusion

The above data presents that a mixture of organic chemicals we produced from the irradiation of the ethanol suspension of the catalyst. Prior art hypothesizes that the mixture is composed of ammonia, formaldehyde, acetaldehyde, and acetone (Gao et. al., 2018). More work is needed to describe the chemical evolution with time, but these results are a first step and demonstrate that gamma-catalyst mediated reactions are possible.

4.0 References

- Bao, Jian–Zhao, Halidan Maimaiti, Xu-wei Zhao, Jin-yan Sun, and Li-rong Feng. "Preparation and immobilisation of Brookite-type Ti³⁺-TiO₂ for photocatalytic ammonia synthesis from N₂ and H₂O." *Applied Surface Science* 602 (2022): 154328. <https://doi.org/10.1016/j.apsusc.2022.154328>
- Chen, Cai, Jiewei Chen, Zhiyuan Wang, Fei Huang, Jian Yang, Yunteng Qu, Kuang Liang et al. "Surface Brønsted-Lewis dual acid sites for high-efficiency dinitrogen photofixation in pure water." *Journal of Energy Chemistry* 67 (2022): 824-830. <https://doi.org/10.1016/j.jechem.2021.10.039>
- Chen, Xingzhu, Neng Li, Zhouzhou Kong, Wee-Jun Ong, and Xiujian Zhao. "Photocatalytic fixation of nitrogen to ammonia: state-of-the-art advancements and future prospects." *Materials Horizons* 5, no. 1 (2018): 9-27. <https://doi.org/10.1039/C7MH00557A>
- Fernandez, C. A., & Hatzell, M. C. (2020). Editors' Choice—Economic Considerations for Low-Temperature Electrochemical Ammonia Production: Achieving Haber-Bosch Parity. *Journal of The Electrochemical Society*, 167(14), 143504. <https://doi.org/10.1149/1945-7111/abc35b>
- Foster, S. L., Bakovic, S. I. P., Duda, R. D., Maheshwari, S., Milton, R. D., Minter, S. D., Janik, M. J., Renner, J. N., & Greenlee, L. F. (2018). Catalysts for nitrogen reduction to ammonia. *Nature Catalysis*, 1(7), 490–500. <https://doi.org/10.1038/s41929-018-0092-7>
- Gao, Xiang, Yuanjing Wen, Dan Qu, Li An, Shiliang Luan, Wenshuai Jiang, Xupeng Zong, Xingyuan Liu, and Zaicheng Sun. "Interference effect of alcohol on Nessler's reagent in photocatalytic nitrogen fixation." *ACS Sustainable Chemistry & Engineering* 6, no. 4 (2018): 5342-5348. <https://doi.org/10.1021/acssuschemeng.8b00110>
- Li, Chang, MengZhen Gu, MingMing Gao, KeNing Liu, XinYu Zhao, NaiWen Cao, Jing Feng, YueMing Ren, Tong Wei, and MingYi Zhang. "N-doping TiO₂ hollow microspheres with abundant oxygen vacancies for highly photocatalytic nitrogen fixation." *Journal of Colloid and Interface Science* 609 (2022): 341-352. <https://doi.org/10.1016/j.jcis.2021.11.180>
- Liu, Chuangwei, Qinye Li, Jie Zhang, Yonggang Jin, Douglas R. MacFarlane, and Chenghua Sun. "Conversion of dinitrogen to ammonia on Ru atoms supported on boron sheets: a DFT study." *Journal of Materials Chemistry A* 7, no. 9 (2019): 4771-4776. <https://doi.org/10.1039/C8TA08219G>
- Mohamed, Amro MO, and Yusuf Bicer. "The Search for Efficient and Stable Metal-Organic Frameworks for Photocatalysis: Atmospheric Fixation of Nitrogen." *Applied Surface Science* 583 (2022): 152376. <https://doi.org/10.1016/j.apsusc.2021.152376>

- Razon, Luis F. "Life cycle analysis of an alternative to the haber-bosch process: Non-renewable energy usage and global warming potential of liquid ammonia from cyanobacteria." *Environmental Progress & Sustainable Energy* 33, no. 2 (2014): 618-624. <https://doi.org/10.1002/ep.11817>
- Song, Guangxin, Rui Gao, Zhao Zhao, Yujun Zhang, Huaqiao Tan, Haibo Li, Dandan Wang, Zaicheng Sun, and Ming Feng. "High-spin state Fe (III) doped TiO₂ for electrocatalytic nitrogen fixation induced by surface F modification." *Applied Catalysis B: Environmental* 301 (2022): 120809. <https://doi.org/10.1016/j.apcatb.2021.120809>
- Shi, Lei, Yu Yin, Shaobin Wang, and Hongqi Sun. "Rational catalyst design for N₂ reduction under ambient conditions: strategies toward enhanced conversion efficiency." *ACS Catalysis* 10, no. 12 (2020): 6870-6899. <https://doi.org/10.1021/acscatal.0c01081>
- Valera-Medina, A., Amer-Hatem, F., Azad, A. K., Dedoussi, I. C., De Joannon, M., Fernandes, R. X., Glarborg, P., Hashemi, H., He, X., Mashruk, S., McGowan, J., Mounaim-Rouselle, C., Ortiz-Prado, A., Ortiz-Valera, A., Rossetti, I., Shu, B., Yehia, M., Xiao, H., & Costa, M. (2021). Review on ammonia as a potential fuel: From synthesis to economics. *Energy and Fuels*, 35(9), 6964–7029. <https://doi.org/10.1021/acs.energyfuels.0c03685>
- Wang, Miao, Mohd A. Khan, Imtihan Mohsin, Joshua Wicks, Alexander H. Ip, Kazi Z. Sumon, Cao-Thang Dinh, Edward H. Sargent, Ian D. Gates, and Md Golam Kibria. "Can sustainable ammonia synthesis pathways compete with fossil-fuel based Haber–Bosch processes?." *Energy & Environmental Science* 14, no. 5 (2021): 2535-2548. <https://doi.org/10.039/DOEE03808C>
- Xue, Xiaolan, Rengeng Chen, Changzeng Yan, Peiyang Zhao, Yi Hu, Wenjun Zhang, Songyuan Yang, and Zhong Jin. "Review on photocatalytic and electrocatalytic artificial nitrogen fixation for ammonia synthesis at mild conditions: Advances, challenges and perspectives." *Nano Research* 12, no. 6 (2019): 1229-1249. <https://doi.org/10.1007/s12274-018-2268-5>
- Zhang, Shuai, Yunxuan Zhao, Run Shi, Geoffrey IN Waterhouse, and Tierui Zhang. "Photocatalytic ammonia synthesis: Recent progress and future." *EnergyChem* 1, no. 2 (2019): 100013. <https://doi.org/10.1016/j.enchem.2019.100013>
- Zhang, L., Chuaicham, C., Balakumar, V., & Sasaki, K. (2022). Effect of ionic Fe (III) doping on montmorillonite for photocatalytic reduction of Cr (VI) in wastewater. *Journal of Photochemistry and Photobiology A: Chemistry*, 429, 113909. <https://doi.org/10.1016/j.jphotochem.2022.113909>
- Zhao, Weirong, Jing Zhang, Xi Zhu, Meng Zhang, Jing Tang, Min Tan, and Yan Wang. "Enhanced nitrogen photofixation on Fe-doped TiO₂ with highly exposed (1 0 1) facets in

the presence of ethanol as scavenger." *Applied Catalysis B: Environmental* 144 (2014): 468-477. <https://doi.org/10.1016/j.apcatb.2013.07.047>

Zhao, Yunxuan, Run Shi, Xuanang Bian, Chao Zhou, Yufei Zhao, Shuai Zhang, Fan Wu et al. "Ammonia detection methods in photocatalytic and electrocatalytic experiments: how to improve the reliability of NH₃ production rates?." *Advanced Science* 6, no. 8 (2019): 1802109. <https://doi.org/10.1002/advs.201802109>

Appendix: Ion Selective Electrode Incompatibility

An issue with the ion selective electrode came with the reproducibility of check standards. Upon calibration with 5, 10, 25, 50, and 100 $\mu\text{g/mL}$ standards, the solution of 25 $\mu\text{g/mL}$ was run, and the ammonia concentration ranged from 15 to 30 $\mu\text{g/mL}$. The reproducibility was completely unreliable and the results are displayed in Figure 18.

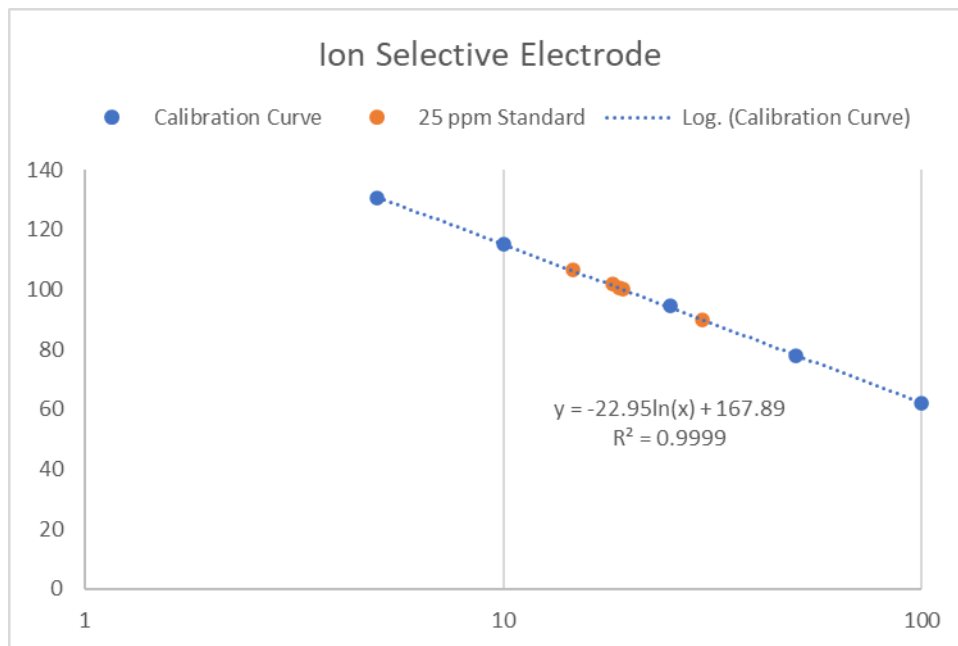


Figure 18: Results from the ion selective electrode study looking at reproducibility of a single standard with multiple analysis is displayed

Pacific Northwest National Laboratory

902 Battelle Boulevard
P.O. Box 999
Richland, WA 99354
1-888-375-PNNL (7665)

www.pnnl.gov